EPJ B
Condensed Matter and Complex Systems
www.epj.org

Eur. Phys. J. B **66**, 165–169 (2008) DOI: 10.1140/epjb/e2008-00393-4

Extended modes and energy dynamics in two-dimensional lattices with correlated disorder

F.A.B.F. de Moura and F. Domínguez-Adame

EDP SCIENCES
Società Italiana di Fisica
Springer

Eur. Phys. J. B **66**, 165–169 (2008)
DOI: 10.1140/epjb/e2008-00393-4

THE EUROPEAN PHYSICAL JOURNAL B

Extended modes and energy dynamics in two-dimensional lattices with correlated disorder

F.A.B.F. de Moura[1,a] and F. Domínguez-Adame[2]

[1] Instituto de Física, Universidade Federal de Alagoas, Maceió AL 57072-970, Brazil
[2] GISC, Departamento de Física de Materiales, Universidad Complutense, E-28040 Madrid, Spain

Received 27 August 2008 / Received in final form 29 September 2008
Published online 24 October 2008 –

Abstract. We study the nature of the vibrational modes in a two-dimensional harmonic lattice with long-range correlated random masses, with power-law spectral density $S(k) \sim 1/k^{\alpha}$. We obtain numerically the scale invariance of the fluctuations of the relative participation number and the local density of states. We find signatures of extended vibrational modes when $\alpha > \alpha_c$ and α_c depends on the magnitude of disorder. In order to confirm this claim, we also study the time evolution of an initially localized perturbation of the lattice. We show that the second moment of the spatial distribution of the energy displays a ballistic regime when $\alpha > \alpha_c$, in agreement with the occurrence of extended vibrational modes.

PACS. 74.25.Kc Phonons – 73.23.Ad Ballistic transport – 73.20.Jc Delocalization processes – 72.15.Rn Localization effects (Anderson or weak localization)

1 Introduction

Spatial localization of collective excitations by a random potential is a quite general feature of classical and quantum systems [1]. Most vibrational modes of one-dimensional (1D) harmonic chains with a random sequence of masses are localized [2]. However, there are a few low-frequency modes not localized, whose number is of the order of $\sqrt{N}$, N being the number of masses in the chain [2,3]. Besides these low-frequency extended modes, short-range correlations in the spring constants [4] and masses [5] lead to a new set of non-scattered modes. Among models with short-range correlation, 1D chains with diluted disorder also support extended modes [6]. The model consists of two interpenetrating sub-lattices, one composed of random masses and the other being periodic. Due to the periodicity of one sub-lattice, special resonant energies appear, giving rise to a set of extended states. In addition, the effect of long-range correlated disorder on the transport properties in low dimensional system has attracted much interest. In general, extended states for 1D potentials with long-range correlations was predicted [7] and experimentally verified in a microwave waveguide with intentionally introduced correlated disorder [8].

Moreover, the two-dimensional (2D) Anderson model under the presence of isotropic scale-free long-range correlated disorder was investigated in detail [9]. By using a single parameter scaling hypothesis the phase diagram and the critical correlation length exponent were estimated [9]. More recently, a reduction of the localization length due to specific long-range correlations in random potentials was experimentally observed [10]. Using a single mode wave-guide, a strong decrease of the localization length was observed when white-noise scatterers are replaced by a correlated arrangement of scatterers. In harmonic systems, it was numerically proven that when the sequence of masses is long-range correlated, with a power law spectral density $S(k) \sim 1/k^{\alpha}$, a phase of extended modes emerges, provided $\alpha > 1$ [11].

In this work we study 2D harmonic lattices with masses exhibiting long-range correlated disorder, $S(k) \sim 1/k^{\alpha}$. We focus on the participation number and its fluctuations, as well as the local density of modes within the band of allowed frequencies. We find extended vibrational modes in the low-frequency region for $\alpha > \alpha_c$, where α_c depends on the magnitude of disorder. The dynamics of an initially localized excitation is also studied by computing the second moment of the energy distribution. We find that, associated with the emergence of a phase of delocalized modes, a ballistic regime takes place.

2 Physical model

We start by considering a 2D disordered harmonic lattice of $N \times N$ masses, for which the classical Hamiltonian can be written as $H = \sum_{n,m} h_{n,m}(t)$, where the energy

[a] e-mail: fidelis@if.ufal.br

$h_{n,m}(t)$ of the mass at site (n,m) is given by

$$h_{n,m}(t) = \frac{P_{n,m}^2}{2m_{n,m}} + \frac{1}{4}\Big[(Q_{n+1,m}-Q_{n,m})^2 + (Q_{n,m}-Q_{n-1,m})^2 + (Q_{n,m+1}-Q_{n,m})^2 + (Q_{n,m}-Q_{n,m-1})^2\Big] . \quad (1)$$

Here $P_{n,m}$ and $Q_{n,m}$ define the momentum and displacement of the mass at site (n,m). In our calculations, we will use units where all elastic couplings are set to unity. By considering only longitudinal displacements and inserting a solution of the form $Q_{n,m} = u_{n,m}\exp(i\omega t)$ we obtain the following equation of motion

$$\Big(4-\omega^2 m_{n,m}\Big)u_{n,m} = u_{n-1,m}+u_{n+1,m} + u_{n,m+1}+u_{n,m-1} . \quad (2)$$

After defining $u_{n,m} = c_{n,m}/\sqrt{m_{n,m}}$ we get

$$\left(\frac{4}{m_{n,m}}-\omega^2\right)c_{n,m} = \frac{c_{n-1,m}}{\sqrt{m_{n,m}m_{n-1,m}}} + \frac{c_{n+1,m}}{\sqrt{m_{n,m}m_{n+1,m}}} + \frac{c_{n,m+1}}{\sqrt{m_{n,m}m_{n,m+1}}} + \frac{c_{n,m-1}}{\sqrt{m_{n,m}m_{n,m-1}}} . \quad (3)$$

In order to generate a long-range correlated sequence of masses, we apply a 2D discrete Fourier transform method. We define a random mass variable as $m_{n,m} = \sigma\tanh(\zeta_{n,m})+\mu$ where

$$\zeta_{n,m} = \sum_{k_n,k_m=1}^{N/2} \frac{1}{(k_n^2+k_m^2)^{\alpha/4}} \cos\left(2\pi\frac{nk_n}{N}+\psi_{n,m}\right) \times \cos\left(2\pi\frac{mk_m}{N}+\phi_{n,m}\right) . \quad (4)$$

$\psi_{n,m}$ and $\phi_{n,m}$ are $N^2/2$ independent random phases uniformly distributed in the interval $[0,2\pi]$. The parameters σ and μ are chosen to have $\langle m_{n,m}\rangle = \Delta = 1$ and $\langle m_{n,m}^2\rangle = 2$ to avoid negative masses. This sequence is the trace of a 2D fractional Brownian motion with a power-law spectral density $S(k)\propto 1/k^\alpha$, where $k=\sqrt{k_n^2+k_m^2}$ [9,12]. In the case $\alpha\to 0$ one recovers the Anderson model with uncorrelated disorder. The opposite limit $\alpha\to\infty$ is analogous to a tight-binding model with a harmonic potential. Intermediate values of α give rise to a long-range correlated sequence of masses.

2.1 Eigenmodes

The vibrational modes can be found by exact diagonalization of the secular matrix of coefficients $c_{n,m}$. In our calculations we compute the average of the participation number, defined by [11]

$$\xi(\omega^2) = \sum_{n,m=1}^{N} c_{n,m}^2(\omega^2) \Big/ \sum_{n,m=1}^{N} c_{n,m}^4(\omega^2) . \quad (5)$$

In general the participation number is a good estimate of the number of sites that participate in the oscillation. For extended states, ξ is proportional to the total number of sites ($\xi\propto N^2$ for a square lattice). We will be also interested in the relative fluctuation of the participation number given by

$$\eta(\omega^2) = \sqrt{\langle\xi^2(\omega^2)\rangle/\langle\xi(\omega^2)\rangle^2 - 1} . \quad (6)$$

Within the framework of random and non-random long-range hopping models, it was demonstrated rigorously that the distribution function of the participation function is scale invariant at the Anderson transition [13]. Such scale invariance has been used to monitor the critical point of long-range hopping models [14]. Within the framework of the single parameter scaling hypothesis [9], the relative fluctuation η at the vicinity of the mobility edge can be written in the form $\eta(\omega^2) = g[(\omega^2-\omega_c^2)N^{1/\nu}]$, which reflects the scale invariance of the participation number distribution at the critical point on which the relative fluctuation assumes the value $g(0)$ irrespective of the system size. We will employ a finite size scaling analysis to estimate the critical exponent ν which governs the scaling behavior of the relevant length scale at the vicinity of the mobility edge, i.e., $l_\infty\propto|\omega-\omega_c|^{-\nu}$. According to the above scaling hypothesis, the derivative $\delta = \partial\eta(\omega^2)/\partial\omega^2$ shall scale at the vicinity of the critical point as $\delta = N^{1/\nu}f[(\omega^2-\omega_c^2)N^{1/\nu}]$. At the mobility edge $\omega=\omega_c$, δ scales with the system size as a power-law $N^{1/\nu}$ from which the critical exponent ν can be directly estimated.

We also consider the local density of states (LDOS) [15]

$$\rho_{n,m}(\omega^2) = \Big\langle \sum_\beta |c_{n,m}(\omega_\beta^2)|^2\,\delta(\omega^2-\omega_\beta^2)\Big\rangle , \quad (7)$$

where the sum runs over the eigenmodes β of the lattice. Averaging $\rho_{n,m}(\omega^2)$ arithmetically over $N\times N$ sites we obtain the averaged density of states

$$\rho_a(\omega^2) = \frac{1}{N^2}\sum_{n,m=1}^{N}\rho_{n,m}(\omega^2) . \quad (8)$$

The geometric mean of the LDOS is defined as

$$\rho_g(\omega^2) = \exp\left[\frac{1}{N^2}\sum_{n,m=1}^{N}\ln\rho_{n,m}(\omega^2)\right] . \quad (9)$$

For extended states, $\rho_a(\omega^2)$ and $\rho_g(\omega^2)$ are almost equal, whereas for localized states $\rho_g(\omega^2)$ vanishes and $\rho_a(\omega^2)$ remains finite [15]. This implies that the ratio

$$R(\omega^2) = \rho_g(\omega^2)/\rho_a(\omega^2) \quad (10)$$

can be used to monitor extended states ($R>0$) and localized ones ($R\to 0$).

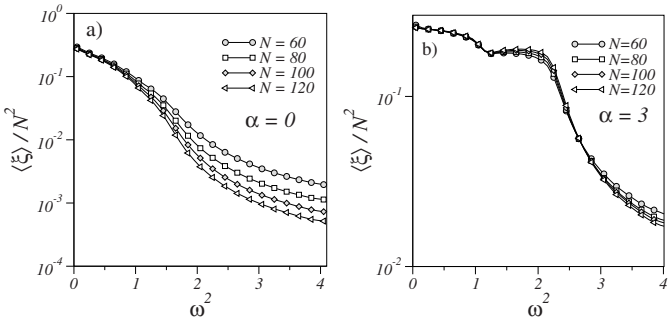

Fig. 1. Finite size scaling of the normalized participation number versus ω^2 for (a) $\alpha = 0$ and (b) $\alpha = 3$.

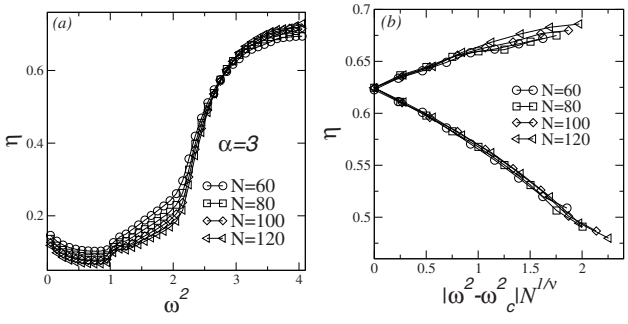

Fig. 2. (a) Relative fluctuation of the participation number versus ω^2 for $\alpha = 3$. (b) Near the critical frequency all data collapse in a universal scaling form indicating the accuracy of the estimated correlation length exponent.

2.2 Energy transport

The fraction of the total energy H_0 at the site (n, m) is given by $h_{n,m}(t)/H_0$ and the second moment of the energy distribution, $M_2(t)$, is defined by [16]

$$M_2^2(t) = \sum_{n,m=1}^{N} \left\{ \left[n - \widetilde{n}(t)\right]^2 + \left[m - \widetilde{m}(t)\right]^2 \right\} \frac{h_{n,m}(t)}{H_0} \,, \quad (11)$$

where an initial excitation is introduced at site (n_0, m_0), $\widetilde{n}(t) = \sum_{n,m=1}^{N} n h_{n,m}(t)/H_0$ and $\widetilde{m}(t)$ is defined similarly. The second moment of the energy distribution (11) has the same status of the mean-square displacement of the wave packet of an electron in a solid [16]. In a disordered three-dimensional system with extended states, the obtained dynamics is in general diffusive. However, in 1D harmonic system with strong correlations in the mass distribution, $M_2^2(t)$ have shown to have ballistic behavior.

3 Results

Eigenmodes and eigenfrequencies were obtained by direct diagonalization of the equation for the amplitudes $c_{n,m}$, equation (3), using lattices up to $N \times N = 120 \times 120$ sites with rigid boundary conditions. From them, the participation number (5) and its relative fluctuation (6) were calculated. Results were obtained after averaging over 1000 realizations of the random sequence of masses. The error bars obtained were less than the symbols size.

Figure 1a shows the scaled average participation number $\langle \xi \rangle / N^2$ as a function of ω^2 for $\alpha = 0$ and $N \times N = 60 \times 60$ up to 120×120. One can see that the average participations number scales proportional to the number of masses N^2 only when $\omega \to 0$. For vibrational modes with $\omega > 0$, $\langle \xi \rangle / N^2 \to 0$ as N diverges, thus indicating that vibrational modes are spatially localized. This trend changes dramatically when correlations in the random sequence of masses are strong. In Figure 1b we show the results for $\alpha = 3$. The well defined data collapse in the low-frequency region $[\xi(\omega < \omega_c) \propto N^{1.98(4)}]$ suggests the existence of extended modes over a finite frequency range. The minimum between $1 < \omega^2 < 2$ is reminiscent from the pure case ($m_{n,m} = m_0$, not shown in the figure).

To determine accurately the value of the frequency separating the phase of extended modes from the localized ones (hereafter referred to as *mobility edge* by analogy with the electronic case), we have calculated the relative fluctuation of the participation number, $\eta(\omega^2)$. In Figure 2 we display $\eta(\omega^2)$ for the same set of parameters of Figure 1b. At the top of the frequency band, the relative fluctuation increase with the system size due to the exponential localization of the eigenstates. On the contrary, at the low-frequency part of the frequency band, the relative fluctuation decreases by increasing the system size, signaling the occurrence of extended modes. Notice that the relative fluctuations are independent of the system size at the critical frequency $\omega_c^2 = 2.9(1)$. This critical frequency can be identified as the mobility edge mentioned above. This value is consistent with the range of frequencies displaying a quadratic scaling of the participation function with the data collapse seen in Figure 1a. In Figure 1b, the relative fluctuation of the participation function $\eta(\omega^2)$ near the critical frequency for $\alpha = 3$ versus the scaling variable $|\omega^2 - \omega_c^2| N^{1/\nu}$, with $\nu = 2.70(15)$. All data collapse in a universal scaling curve, indicating the accuracy of the estimated correlation length exponent. Upper and lower branches correspond, respectively, to exponentially localized and extended states. We have obtained the exponent $\nu = 2.10(20)$ for $\alpha = 2.5$. For larger values of α, the numerical estimate of the derivative becomes less confident, once the mobility edge approaches the band edge and the vanishing small density of states near the extremal of the energy band degrades the statistical averages, thus resulting in larger error bars.

The existence of a mobility edge is further supported by the behavior of the ratio $R(\omega^2)$ given by (10). Figure 3 shows this ratio when $N \times N = 120 \times 120$ and $\alpha = 3$. The δ-function in equation (7) was computed as a normalized box function of width 0.01. One can see from these calculations that the function $R(\omega^2)$ becomes large in the frequency range $\omega^2 < \omega_c^2$. This is again a signature of extended states in this frequency region. On the contrary, $R(\omega^2)$ is vanishingly small when $\omega^2 < \omega_c^2$. Therefore, the results from the average participation number, its fluctuations and the LDOS lead to the conclusion that there

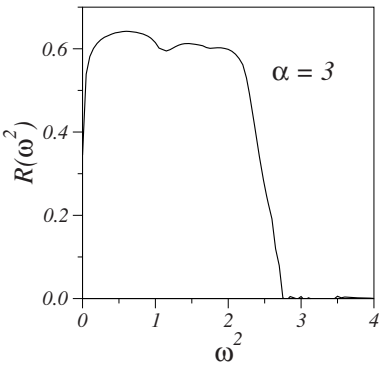

Fig. 3. (a) Ratio R versus ω^2 for $N \times N = 120 \times 120$ and $\alpha = 3$.

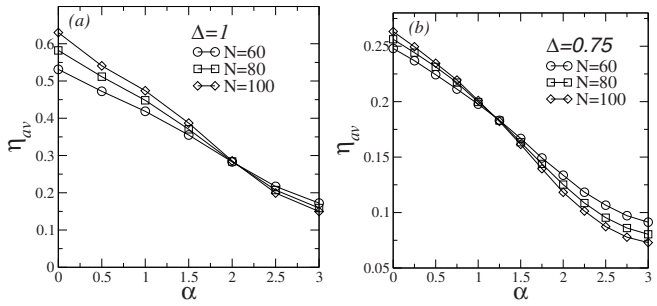

Fig. 4. (a)Relative fluctuation of the participation number, averaged over a frequency window $0.5 < \omega^2 < 1.5$, versus α for (a) $\Delta = 1$ and (b) $\Delta = 0.75$.

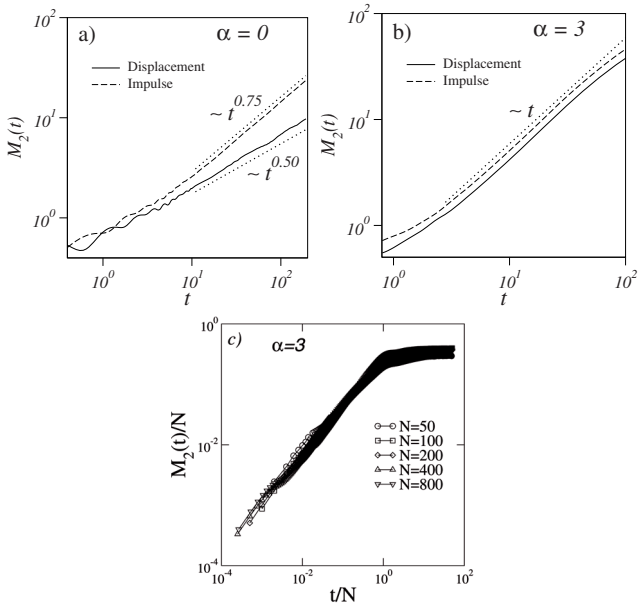

Fig. 5. Second moment of the energy distribution versus time for a lattice size $N \times N = 10^3 \times 10^3$ obtained by using impulse (dashed line) and displacement (solid line) initial excitations, for (a) $\alpha = 0$ and (b) $\alpha = 3$. Dotted lines are guides to the eye. (c) Scaled second moment of the energy distribution $M_2(t)/N$ versus scaled time t/N computed from lattices with $N = 50$ up to 800 and $\alpha = 3$.

exists a phase of extended modes with frequency smaller than ω_c.

As mentioned in the previous paragraph, the relative fluctuation of the participation number is an excellent tool to determine accurately the mobility edge. The existence of extended states have been observed when the correlation exponent α is large. We make use of this tool to elucidate the critical exponent α_c above which the phase of extended state appears. To this end, we have averaged the relative fluctuation of the participation number over a frequency window $0.5 < \omega^2 < 1.5$, η_{av}. Figure 4a shows the average relative fluctuation η_{av} as a function of the correlation exponent α. η_{av} becomes independent of the system size when the correlation exponent is about 2. Thus, we can estimate that $\alpha_c \simeq 2$. Before concluding, some words concerning the critical value α_c and its relations with the mass distribution parameters are in order. In reference [17], it was numerically proven that in 1D electronic system with long-range correlated disorder, the critical correlation exponent α_c is rather independent on the magnitude of disorder Δ. In Figure 4b we show the same results as in Figure 4a but for $\Delta = 0.75$. We can see that, in this 2D harmonic system, the critical correlation exponent is not universal, but depends on the magnitude of disorder.

Concerning dynamical magnitudes, $\widetilde{n}(t)$, $\widetilde{m}(t)$ and $M_2(t)$, they were obtained by solving numerically the Hamilton equations for $P_{n,m}(t)$ and $Q_{n,m}(t)$. Integration in time was performed using a fourth-order Runge-Kutta method with time step 10^{-3} and systems up to $N \times N = 10^3 \times 10^3$ sites. Energy conservation was used to check numerical accuracy at every time step. Two kind of initial conditions were used to integrate the equation of motion. *Impulse* excitations correspond to $P_{n,m}(t = 0) = P_0\, \delta_{n,N/2}\, \delta_{m,N/2}$ and $Q_{n,m}(t = 0) = 0$. Similarly, *displacement* excitations correspond to $Q_{n,m}(t = 0) = Q_0\, \delta_{n,N/2}\, \delta_{m,N/2}$ and $P_{n,m}(t = 0) = 0$.

In Figure 5a we plot the second moment $M_2(t)$ as a function of time for a 2D uncorrelated harmonic lattice ($\alpha = 0$), for both impulse (dashed line) and displacement (solid line) initial excitations. The dynamics behavior obtained, $M_2(t) \propto t^{0.75}$ for *impulse* initial excitation and $M_2(t) \propto t^{0.5}$ is similar to that found in reference [16]. In fact, in random harmonic chains with an initial impulse excitation, the energy spread is faster than that for an initial displacement excitation [16,18]. This scenario is consistent with the absence of extended modes. Figure 5b indicates that long-range correlations in the sequence of masses ($\alpha = 3$) induce a ballistic behavior, i.e., $M_2(t) \propto t^1$ independent of the kind of initial excitation. These results provide further support to the occurrence of extended modes in long-range correlated lattices. We further collected in Figure 5c results for the scaled second moment of the energy distribution $M_2(t)/N$ versus scaled time t/N computed from lattices with $N = 50$ up to 800 and $\alpha = 3$. We numerically integrate the equation until a stationary state can be reached after multiple reflections of the energy pulse on the lattice boundaries. Therefore, $M_2(t) \propto N$ due to finite size effects. A good

data collapse for long time is found, implying that the energy pulse spread ballistic before reaching the lattice boundaries, in perfect agreements with Figure 5b.

4 Conclusions

We have studied the nature of vibrational modes in 2D harmonic lattices with masses exhibiting long-range correlated disorder with spectral density proportional to $1/k^{\alpha}$. By direct diagonalization of the equation of motion, we have computed the participation number ξ and its fluctuations η. When $\alpha = 0$, corresponding to the uncorrelated sequence of masses, the magnitude $\langle\xi\rangle/N^2$ becomes independent of the number of masses N^2 only when $\omega \to 0$. Remarkably, when correlations in the disorder are strong ($\alpha > \alpha_c$), the curves $\langle\xi\rangle/N^2$ as functions of ω^2 for different values of N^2 collapse onto a single curve over a broad frequency interval $[0, \omega_c]$. Thus we claim that vibrational modes whose frequency lies within this range are truly extended. The critical frequency ω_c can be accurately determined from the size invariance of the relative fluctuation η. The critical value α_c is strongly dependent on the kind of mass distribution. Using a finite-size scaling hypothesis, we obtained a data collapse from different system sizes close to the critical point of the localized-delocalized transition in the regime of $\alpha > \alpha_c$. The critical correlation exponent was estimated to be $\nu = 2.10(20)$ for $\alpha = 2.5$ and $\nu = 2.70(20)$ for $\alpha = 3.0$, indicating that the correlation length exponent is nonuniversal.

In order to study the time evolution of an initially localized energy input, we calculated the second moment $M_2(t)$ of the energy spatial distribution. We have shown that $M_2(t)$, besides being dependent of the specific initial excitation and exhibiting an anomalous diffusion for weakly correlated disorder, assumes a ballistic spread in the range $\alpha > 2$ due to the presence of extended vibrational modes. The presence of new extended modes at low frequencies and the anomalous energy spreading indicate that the thermal conductivity [19] can be strongly influenced by the existence of long-range correlated mass distribution.

Work at Brazil was supported by Federal Brazilian Agencies (CNPq, CAPES, and FINEP) and Alagoas State Agencies (CNPq–Rede Nanobioestruturas and FAPEAL). Work at Madrid was supported by BSCH-UCM (Project PR34/07-15916) and MEC (Project FIS2006-01485).

References

1. E. Abrahams, P.W. Anderson, D.C. Licciardello, T.V. Ramakrishnan, Phys. Rev. Lett. **42**, 673 (1979). For a review see, e.g., I. M. Lifshitz, S.A. Gredeskul, L.A. Pastur, *Introduction to the Theory of Disordered Systems* (Wiley, New York, 1988)
2. P. Dean, Proc. Phys. Soc. **84**, 727 (1964)
3. H. Matsuda, K. Ishii, Prog. Theor. Phys. Suppl. **45**, 56 (1970); K. Ishii, Prog. Theor. Phys. Suppl. **53**, 77 (1973)
4. F. Domínguez-Adame, E. Maciá, A. Sánchez, Phys. Rev. B **48**, 6054 (1993)
5. P.K. Datta, K. Kundu, J. Phys.: Condens. Matter **6**, 4465 (1994)
6. S.S. Albuquerque, F.A.B.F. de Moura, M.L. Lyra, Physica A **357**, 165 (2005)
7. F.A.B.F. de Moura, M.L. Lyra, Phys. Rev. Lett. **81**, 3735 (1998); F.A.B.F. de Moura, M.L. Lyra, Phys. Rev. Lett. **84**, 199 (2000)
8. U. Kuhl, F.M. Izrailev, A. Krokhin, H.J. Stöckmann, Appl. Phys. Lett. **77**, 633 (2000)
9. I.F. dos Santos, F.A.B.F. de Moura, M.D. Coutinho-Filho, M.L. Lyra, J. Phys.: Condens. Matter **19**, 476213 (2007)
10. U. Kuhl, F.M. Izrailev, A. Krokhin , Phys. Rev. Lett. **100**, 126402 (2008)
11. F.A.B.F. de Moura, M.D. Coutinho-Filho, E.P. Raposo, M.L. Lyra, Phys. Rev. B **68**, 012202 (2003)
12. D.R. McGaughey, G.J.M. Aitken, Physica A **311**, 369 (2002)
13. F. Evers, A.D. Mirlin, Phys. Rev. Lett. **84**, 3690 (2000); F. Evers, A.D. Mirlin, Phys. Rev. Lett. Phys. Rev. B **62**, 7920 (2000)
14. A.V. Malyshev, V.A. Malyshev, F. Domínguez-Adame, Phys. Rev. B **70**, 172202 (2004)
15. A. Alvermann, H. Fehske, Eur. Phys. J. B **48**, 295 (2005)
16. P.K. Datta, K. Kundu, Phys. Rev. B **51**, 6287 (1995)
17. H. Shima, T. Nomura, T. Nakayama, Phys. Rev. B **70**, 075116 (2004)
18. M. Wagner, G. Zart, J. Vázquez-Márquez, G. Viliani, W. Frizzera, O. Pilla, M. Montagna, Philos. Mag. B **65**, 273 (1992)
19. B. Li, J. Wang, Phys. Rev. Lett. **91**, 044301 (2003)